HHS Public Access

Author manuscript

Biochemistry. Author manuscript; available in PMC 2020 June 25.

Published in final edited form as:

Biochemistry. 2019 June 25; 58(25): 2809–2813. doi:10.1021/acs.biochem.9b00299.

Myristoylation-Dependent Palmitoylation of the Receptor Tyrosine Kinase Adaptor FRS2α

Barbara Barylko[†], **Yu-Ju Chen**[‡], **Jared Hennen**[§], **Isaac Angert**[§], **Yan Chen**[§], **Joachim D. Mueller**[§], **Hui-Qiao Sun**[‡], **Clinton A. Taylor IV**[†], **Jen Liou**[‡], **Helen Yin**[‡], **Joseph P. Albanesi**[*,†]

[†]Department of Pharmacology, University of Texas Southwestern Medical Center, 6001 Forest Park, Dallas, Texas 75390, United States

[‡]Department of Physiology, University of Texas Southwestern Medical Center, 6001 Forest Park, Dallas, Texas 75390, United States

[§]School of Physics and Astronomy, University of Minnesota, Minneapolis, Minnesota 55455, United States

Abstract

An early step in signaling from activated receptor tyrosine kinases (RTKs) is the recruitment of cytosolic adaptor proteins to autophosphorylated tyrosines in the receptor cytoplasmic domains. Fibroblast growth factor receptor substrate 2α (FRS2α) associates via its phosphotyrosine-binding domain (PTB) to FGF receptors (FGFRs). Upon FGFR activation, FRS2α undergoes phosphorylation on multiple tyrosines, triggering recruitment of the adaptor Grb2 and the tyrosine phosphatase Shp2, resulting in stimulation of PI3K/AKT and MAPK signaling pathways. FRS2α also undergoes N-myristoylation, which was shown to be important for its localization to membranes and its ability to stimulate downstream signaling events (Kouhara et al., 1997). Here we show that FRS2α is also palmitoylated in cells and that cysteines 4 and 5 account for the entire modification. We further show that mutation of those two cysteines interferes with FRS2α localization to the plasma membrane (PM), and we quantify this observation using fluorescence fluctuation spectroscopy approaches. Importantly, prevention of myristoylation by introduction of a G2A mutation also abrogates palmitoylation, raising the possibility that signaling defects previously ascribed to the G2A mutant may actually be due to a failure of that mutant to undergo palmitoylation. Our results demonstrate that FRS2α undergoes coupled myristoylation and palmitoylation. Unlike stable cotranslational modifications, such as myristoylation and prenylation, palmitoylation is reversible due to the relative lability of the thioester linkage. Therefore, palmitoylation may provide a mechanism, in addition to phosphorylation, for dynamic regulation of FRS2 and its downstream signaling pathways.

[*]**Corresponding Author:** joseph.albanesi@utsouthwestern.edu. Tel: 214-645-6119. Fax: 214-645-6124.

Author Contributions: J.P.A., B.B., Y.C., H.L., J.L., and J.D.M. were responsible for experimental design. B.B. and C.A.T. performed palmitoylation analysis experiments. Y.J.C. and H.Q.S. performed fluorescence light microscopy localization experiments. I.A., J.H., and Y.C. performed fluorescence fluctuation spectroscopy experiments.

The authors declare no competing financial interest.

Supporting Information

The Supporting Information is available free of charge on the ACS Publications website at DOI: 10.1021/acs.biochem.9b00299.

Experimental procedures and FCS characterization (PDF)

FRS2α is an essential gatekeeper for entry into MAPK and AKT signaling pathways triggered by activation of FGF receptors. It serves a similar, albeit more limited, function in signaling mediated by the neurotrophin-binding receptor tyrosine kinases (RTKs), TrkA and TrkB and RET.[1] In addition, it is apparently important for both PDGF[2] and VEGF[3] signaling in the cardiovascular system, although its mechanism of action in these cases is not entirely clear. FRS2α binds directly to RTKs via its phosphotyrosine-binding (PTB) domain (Figure 1A).

However, unlike other PTB-containing RTK adaptors, such as IRS-1, Shc, and Dok, the FRS2α PTB domain binds constitutively (i.e., independently of receptor tyrosine phosphorylation) to a juxtamembrane motif in FGFRs.[4] Because PTB-RTK interactions are relatively weak, association of PTB-containing adaptors with their receptors requires their prior recruitment to the PM. For example, IRS-1 and Dok utilize pleckstrin homology (PH) domain-phosphoinositide interactions for PM recruitment. FRS2α does not contain a lipid-binding module, but instead was found to undergo N-terminal myristoylation, the cotranslational attachment of a 14-carbon myristoyl chain.[5] A nonmyristoylated mutant, FRS2α^{G2A}, fails to undergo FGF-stimulated tyrosine phosphorylation and, hence, does not fully support FGF-mediated ERK and AKT activation.[5,6] The N-terminal sequence of FRS2α also contains three cysteines predicted to be outstanding targets for palmitoylation, the post-translational attachment of a 16-carbon palmitoyl chain.[7] However, this modification was not detected in the original study of FRS2α myristoylation,[5] nor has it been reported in subsequent investigations of FRS2α. Because FRS2α has been identified in three palmitoyl-proteomes,[8–10] we decided to reinvestigate this issue. Using the acyl-resin-assisted capture (acyl-RAC) procedure (see Supporting Information), we identified both endogenous FRS2α and expressed FRS2α-myc-DDK as potentially palmitoylated proteins in cultured cells (Figure 1B). This result was confirmed by detecting ^{3}H-palmitate incorporation into FRS2α-myc-DDK immunoprecipitated from labeled HeLa cells (Figure 1C). Although these methods do not allow precise quantification of the extent of palmitoylation, results of acyl-RAC suggest that at least 50–70% of FRS2α is palmitoylated.

Three cysteines within the N-terminal region of FRS2α ($_{1}$MGSCCSC$_{7}$) are excellent candidates for palmitoylation. However, our mutational analysis indicates that only cysteines 4 and 5 are acylated in cells (Figure 1D). Of particular importance, the G2A mutation, which prevents myristoylation,[5] also prevented palmitoylation. According to bioinformatics programs,[11,12] mutation of cysteines 4 and 5 to serine is not expected to diminish FRS2α myristoylation. Thus, we confirmed that FRS2α is, indeed, palmitoylated and that its palmitoylation requires prior myristoylation.

We next tested whether inhibition of FRS2α palmitoylation affected its association with cellular membranes. As previously shown,[5] nearly the entire pool of FRS2α^{WT} required detergent for extraction from cell homogenates, whereas FRS2α^{G2A} behaved almost exclusively as a soluble protein, extractible in detergent-free buffers (Figure 2A). Likewise, most of the FRS2$\alpha^{C4,5S}$ mutant was soluble, although a small pool remained membrane-bound even in the presence of 1 M NaCl or 0.2 M Na_2CO_3. Examination of other dually lipidated proteins indicates that myristoylation alone promotes transient association with membranes, while subsequent palmitoylation allows for tighter and more prolonged

membrane anchoring.[13] Thus, we suggest that myristoylation accounts for the slightly greater association of FRS2$\alpha^{C4,5S}$ than FRS2α^{G2A} with membranes.

Numerous palmitoylated proteins are concentrated in cholesterol-rich membrane microdomains, often referred to as lipid rafts,[14] which may serve as receptor signaling platforms on the PM.[15] Enrichment of FRS2α in rafts has been reported.[16] Moreover, this raft distribution is physiologically significant, as the neurotrophin receptor RET is recruited to rafts via its interaction with FRS2α.[17] We found that a pool of FRS2α is associated with rafts in HeLa cells and that this association is lost upon treatment with the palmitoylation inhibitor, 2-bromopalmitate (2-BP) (Figure 2B).

To assess the role of palmitoylation in the subcellular targeting of FRS2α, we localized WT and mutant forms of FRS2α-EGFP in HeLa cells using confocal microscopy (Figure 2C). As previously reported,[5] FRS2α^{WT} was predominantly located on the PM, whereas FRS2α^{G2A} showed diffuse cytoplasmic staining, characteristic for soluble proteins. The proportion of FRS2$\alpha^{C4,5S}$ on the PM was greatly reduced compared to FRS2α^{WT}. However, unlike FRS2α^{G2A}, FRS2$\alpha^{C4,5S}$ showed diffuse cytoplasmic staining as well as association with intracellular organelles.

The extended perinuclear location of FRS2$\alpha^{C4,5S}$-EGFP suggested that this mutant may distribute to the Golgi apparatus and/or the endoplasmic reticulum (ER). Therefore, we tested for colocalization of WT and mutant forms of FRS2α-EGFP with the mCherry-K-RAS tail (a PM marker[18]), mCherry-KDEL (an ER marker), and mCherry-P4M (which recognizes phosphatidylinositol 4-phosphate, a lipid that is particularly enriched in the Golgi[19]). As expected, FRS2α^{WT} codistributed at the cell periphery with the K-RAS tail, particularly on cell surface projections, whereas FRS2α^{G2A} showed minimal colocalization with any of the membrane markers (Figure 3A). FRS2$\alpha^{C4,5S}$ colocalized most extensively with P4M-positive Golgi structures (Figure 3B).

We used fluorescence fluctuation spectroscopy (FFS)[20] to determine quantitatively how lipidation influences the behavior of FRS2α in living U2OS cells. Using fluorescence correlation spectroscopy (FCS), we compared the diffusion times of FRS2α^{G2A}-EGFP and FRS2$\alpha^{C4,5S}$-EGFP. The recovered diffusion time of FRS2α^{G2A}-EGFP was concentration-independent (Figure 4A) and similar to that of cytosolic proteins. In contrast, the diffusion times of FRS2$\alpha^{C4,5S}$-EGFP exhibited a pronounced increase with concentration and were far more scattered than those of FRS2α^{G2A} (Figure 4A). These results demonstrate that cytoplasmic FRS2$\alpha^{C4,5S}$, unlike FRS2α^{G2A}, interacts with low-mobility intracellular components in a concentration-dependent manner, perhaps reflecting transient association with membranes. In contrast, FCS on FRS2α^{WT}-EGFP identified a strong PM-bound population with a very low mobility and a minor cytoplasmic population with a high mobility (Figure S1), suggesting strong association with the PM. The cytoplasmic diffusion times of FRS2α^{WT} were close to the corresponding diffusion times for both mutants, indicating the absence of strong membrane association for FRS2α^{G2A} and FRS2$\alpha^{C4,5S}$.

To estimate the relative affinities of WT and mutant FRS2α for the PM, we turned to z-scan FFS.[21] An axial scan of the two-photon focus through the cytoplasm of a cell locally probes

the spatial distribution of a fluorescent protein along the scan path (Figure 4B). The recorded intensity trace from a cell expressing FRS2α^{WT}-EGFP reveals two well-resolved peaks (Figure 4C), which are indicative of a significant population of protein located at the ventral and dorsal PM.[22] We decompose the experimental intensity trace into its components by fitting. The fit identified the fluorescence contributions from each of the two membranes as well as the signal from protein residing within the cytoplasmic space (Figure 4C). A convenient parameter to quantify the signal contributions from the PM is the membrane fraction f_M of the fluorescence intensity, which is defined as the ratio of the peak fluorescence from the membrane divided by the total fluorescence.[23] The membrane fractions in Figure 4C are 75% and 76% for the ventral and dorsal PM, respectively. We performed z-scan FFS on a population of cells and measured at several locations within each cell to acquire a statistical sample of the PM fraction of labeled FRS2α^{WT}. The histogram of the combined PM fractions reveals a significant population of PM-bound FRS2α^{WT} ($f_M > 0.5$) for the z-scan measurements (Figure 4D).

In contrast, the distribution to PM fractions of FRS2$\alpha^{C4,5S}$ EGFP and FRS2α^{G2A}-EGFP shifted to low values ($f_M < 0.5$) (Figure 4E and 4F, respectively), indicating that these mutations result in a significant loss of the PM-bound protein population. Comparison of Figure 4E and 4F indicates that the G2A mutation reduces PM binding more significantly than the C4,5S mutation. The detected PM fractions for FRS2α^{G2A}-EGFP are mostly below 20%. Previous characterization of z-scan FFS established that the lower limit of reliable identification of the PM fraction is between 10 and 20%.[22] To demonstrate this limit, we performed control experiments with GFP. The z-scans identified a distribution of PM fractions (Figure 4G), which is comparable to the distribution observed for FRS2α^{G2A} (Figure 4F). Therefore, we conclude that the binding affinity of FRS2α^{G2A} for the PM has been reduced below our detection limit.

We found that expression levels of FRS2$\alpha^{C4,5S}$ were typically lower than those of FRS2α^{G2A}. To eliminate potential biases in the analysis that could arise from differences in the expression level, we chose a subset of data with matching cytoplasmic concentrations. We chose a narrow concentration range from 20 to 100 nM as the filter and calculated the median and its standard error (Figure 4H). The median of the PM fraction is above 90% for FRS2α^{WT} and reduces to 8 ± 1% for FRS2$\alpha^{C4,5S}$. The median is further reduced to 2.6 ± 0.2% for FRS2α^{G2A}, which is a statistically significant reduction. Similarly, a two-tailed Welch t test determined that the data for FRS2$\alpha^{C4,5S}$ and FRS2α^{G2A} were different ($p < 0.001$). On the other hand, the median PM fraction of FRS2α^{G2A} and the GFP control (2.2% ± 0.5%) are within one standard deviation. This observation is corroborated by a two-tailed t test of these two data sets, which found no significant difference ($p = 0.26$). The results obtained from z-scan measurements are consistent with the FCS experiments of protein mobility (Figure 4A). The C4,5S mutation significantly reduces, but does not eliminate membrane binding. The G2A mutation reduces membrane binding below our detection limit.

Because FGF signaling regulates cell differentiation, growth, survival, and motility, it is not surprising that FRS2α is being actively pursued as a possible therapeutic target in cancer.[24,25] Myristoylation of FRS2α was recently proposed as a promising cancer drug target,

offering the possibility of circumventing the resistance observed with the use of FGFR kinase inhibitors.[6] Our results suggest that protein acyltransferases and thioesterases that regulate FRS2 palmitoylation should also be considered as potential targets for therapeutic intervention in cancer and other growth factor-related diseases.

Supplementary Material

Refer to Web version on PubMed Central for supplementary material.

ACKNOWLEDGMENTS

We thank Jonatan Barylko for the TOC illustration.

Funding

This research was supported by National Institutes of Health (NIH) grants [GM121536 (J.P.A., H.Y., and J.D.M.), GM113079 (J.L., Y-J. C) and GM064589 (Y.C., J.H., and J.D.M.)] and a Basic Science Pilot Grant from the Simmons Comprehensive Cancer Center, UTSW (J.P.A.). I.A. was supported by an NIH grant (T32 AI083196).

ABBREVIATIONS

IRS-1	insulin receptor substrate-1
Shc	Src homology and collagen
Dok	downstream of tyrosine kinases
acyl-RAC	acyl-resin-assisted capture
EGFP	enhanced green fluorescent protein

REFERENCES

(1). Gotoh N (2008) Regulation of growth factor signaling by FRS2 family docking/scaffold adaptor proteins. Cancer Sci. 99, 1319–1325. [PubMed: 18452557]

(2). Chen PY, Simons M, and Friesel R (2009) FRS2 via fibroblast growth factor receptor 1 is required for platelet-derived growth factor receptor beta-mediated regulation of vascular smooth muscle marker gene expression. J. Biol. Chem 284, 15980–15992. [PubMed: 19339244]

(3). Chen PY, Qin L, Zhuang ZW, Tellides G, Lax I, Schlessinger J, and Simons M (2014) The docking protein FRS2α is a critical regulator of VEGF receptors signaling. Proc. Natl. Acad. Sci. U. S.A 111, 5514–5519. [PubMed: 24706887]

(4). Ong SH, Guy GR, Hadari YR, Laks S, Gotoh N, Schlessinger J, and Lax I (2000) FRS2 proteins recruit intracellular signaling pathways by binding to diverse targets on fibroblast growth factor and nerve growth factor receptors. Mol. Cell. Biol 20, 979–989. [PubMed: 10629055]

(5). Kouhara H, Hadari YR, Spivak-Kroizman T, Schilling J, Bar-Sagi D, Lax I, and Schlessinger J (1997) A lipid-anchored Grb2-binding protein that links FGF-receptor activation to the Ras/MAPK signaling pathway. Cell 89, 693–702. [PubMed: 9182757]

(6). Li Q, Alsaidan OA, Ma Y, Kim S, Liu J, Albers T, Liu K, Beharry Z, Zhao S, Wang F, Lebedyeva I, and Cai H (2018) Pharmacologically targeting the myristoylation of the scaffold protein FRS2α inhibits FGF/FGFR-mediated oncogenic signaling and tumor progression. J. Biol. Chem 293, 6434–6448. [PubMed: 29540482]

(7). Zhou F, Xue Y, Yao X, and Xu Y (2006) CSS-Palm: palmitoylation site prediction with a clustering and scoring strategy (CSS). Bioinformatics 22, 894–896. [PubMed: 16434441]

(8). Martin BR, Wang C, Adibekian A, Tully SE, and Cravatt BF (2012) Global profiling of dynamic protein palmitoylation. Nat. Methods 9, 84–89.

(9). Li Y, Martin BR, Cravatt BF, and Hofmann SL (2012) DHHC5 protein palmitoylates flotillin-2 and is rapidly degraded on induction of neuronal differentiation in cultured cells. J. Biol. Chem 287, 523–530. [PubMed: 22081607]

(10). Thinon E, Fernandez JP, Molina H, and Hang HC (2018) Selective enrichment and direct analysis of protein S-palmitoylation sites. J. Proteome Res 17, 1907–1922. [PubMed: 29575903]

(11). Bologna G, Yvon C, Duvaud S, and Veuthey AL (2004) N-terminal myristoylation predictions by ensembles of neural networks. Proteomics 4, 1626–1632. [PubMed: 15174132]

(12). Xie Y, Zheng Y, Li H, Luo X, He Z, Cao S, Shi Y, Zhao Q, Xue Y, Zuo Z, and Ren J (2016) GPS-Lipid: a robust tool for the prediction of multiple lipid modification sites. Sci. Rep 6, 28249. [PubMed: 27306108]

(13). Farazi TA, Waksman G, and Gordon JI (2001) The biology and enzymology of protein N-myristoylation. J. Biol. Chem 276, 39501–39504. [PubMed: 11527981]

(14). Levental I, Grzybek M, and Simons K (2010) Greasing their way: lipid modifications determine protein association with membrane rafts. Biochemistry 49, 6305–6316. [PubMed: 20583817]

(15). Lingwood D, and Simons K (2010) Lipid rafts as a membrane-organizing principle. Science 327, 46–50. [PubMed: 20044567]

(16). Ridyard MS, and Robbins SM (2003) Fibroblast growth factor-2-induced signaling through lipid raft-associated fibroblast growth factor receptor substrate 2 (FRS2). J. Biol. Chem 278, 13803–13809. [PubMed: 12571252]

(17). Lundgren TK, Luebke M, Stenqvist A, and Ernfors P (2008) Differential membrane compartmentalization of Ret by PTB-adaptor engagement. FEBS J. 275, 2055–2066. [PubMed: 18355321]

(18). Heo WD, Inoue T, Park WS, Kim ML, Park BO, Wandless TJ, and Meyer T (2006) PI(3,4,5)P3 and PI(4,5)P2 lipids target proteins with polybasic clusters to the plasma membrane. Science 314, 1458–14561. [PubMed: 17095657]

(19). Hammond GR, Machner MP, and Balla T (2014) A novel probe for phosphatidylinositol 4-phosphate reveals multiple pools beyond the Golgi. J. Cell Biol 205, 113–126. [PubMed: 24711504]

(20). Van Orden A, Fogarty K, and Jung J (2004) Fluorescence fluctuation spectroscopy: a coming of age story. Appl. Spectrosc 58, 122A–137A. [PubMed: 14727729]

(21). Macdonald PJ, Chen Y, Wang X, Chen Y, and Mueller JD (2010) Brightness analysis by Z-scan fluorescence fluctuation spectroscopy for the study of protein interactions within living cells. Biophys. J 99, 979–988. [PubMed: 20682277]

(22). Smith EM, Hennen J, Chen Y, and Mueller JD (2015) Z-scan fluorescence profile deconvolution of cytosolic and membrane-associated protein populations. Anal. Biochem 480, 11–20. [PubMed: 25862080]

(23). Hennen J, Hur KH, Saunders CA, Luxton GWG, and Mueller JD (2017) Quantitative brightness analysis of protein oligomerization in the nuclear envelope. Biophys. J 113, 138–147. [PubMed: 28700912]

(24). Sato T, and Gotoh N (2009) The FRS2 family of docking/scaffolding adaptor proteins as therapeutic targets of cancer treatment. Expert Opin. Ther. Targets 13, 689–700. [PubMed: 19456272]

(25). Luo L, and Hahn WC (2015) Oncogenic Signaling Adaptor Proteins. J. Genet. Genomics 42, 521–529. [PubMed: 26554907]

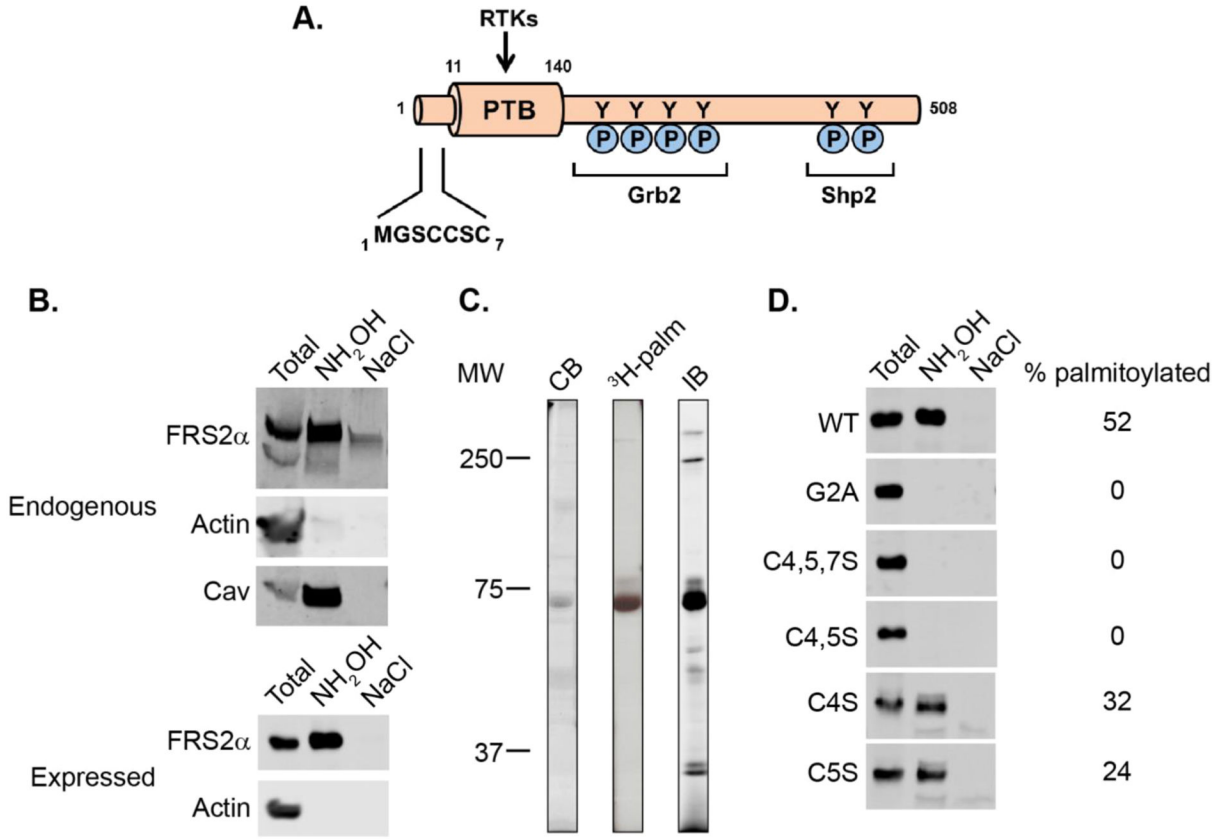

Figure 1.

Palmitolylation of FRS2α. (A) Scheme of human FRS2α showing the N-terminal lipidation motif, RTK-binding PTB domain, and phosphotyrosines that interact with Grb2 and Shp2. (B) Palmitoylation of endogenous FRS2α in HEK293 cells (top) and overexpressed FRS2α-DDK in HeLa cells (bottom) detected by acyl-RAC (see Supporting Information). Actin and caveolin are negative and positive controls, respectively. Total represents 10% of the sample used for analysis. (C) ^{3}H-palmitate incorporation into overexpressed FRS2α-DDK immunoprecipitated with anti-DDK antibodies from ^{3}H-palmitate-labeled HeLa cells. Abbreviations: CB, Coomassie blue-stained gel; ^{3}H-palm, autoradiogram; IB, immunoblot with anti-DDK antibody. (D) Palmitoylation of DDK-tagged FRS2α (WT and mutants) expressed in HeLa cells as detected by acyl-RAC. Total represents 10% of the sample used for analysis.

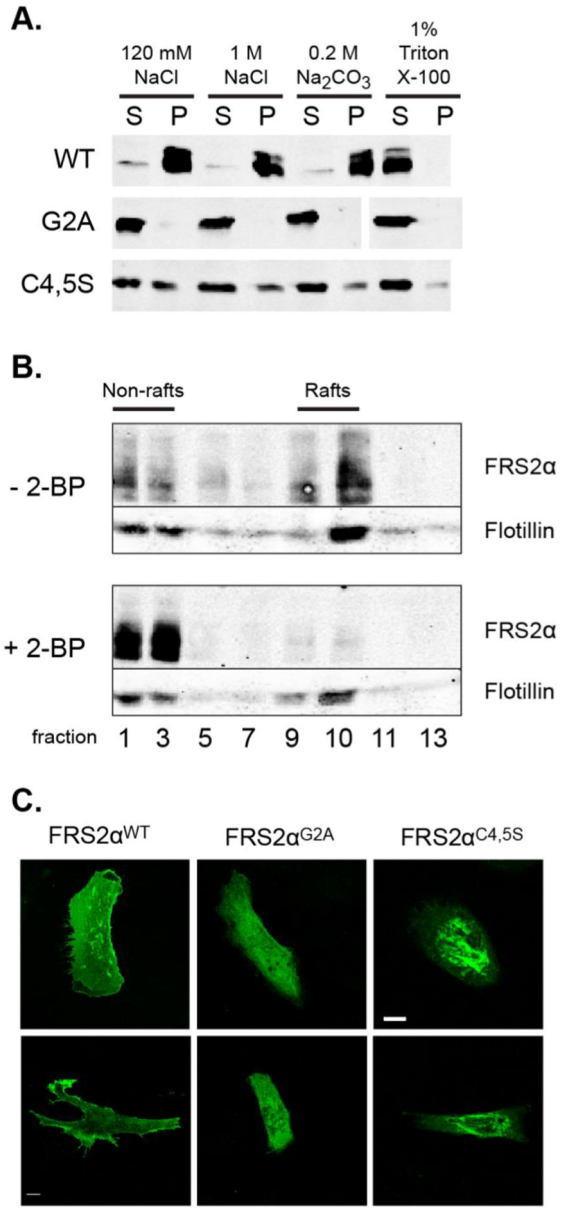

Figure 2.

Effect of disrupting palmitoylation on the solubility and distribution of FRS2α. (A) Effect of mutating lipidated residues on the extractibility of FRS2α. Postnuclear supernatants from HeLa cells expressing FRS2α^{WT}, FRS2α^{G2A}, and FRS2$\alpha^{C4,5S}$ were incubated under the conditions shown and subjected to centrifugation at 210 000g for 15 min to obtain solubilized (S) and particulate (P) fractions. FRS2α was detected with the anti-DDK antibody. (B) Effect of 2-BP on the distribution of overexpressed FRS2α^{WT}-DDK to lipid rafts in HEK293 cells. Flotillin, a raft marker, is stably palmitoylated and is not susceptible to the 6 h 2-BP treatment used in this experiment. (C) Confocal micrographs of HeLa cells expressing FRS2α^{WT}-EGFP (left), FRS2α^{G2A}-EGFP (middle), and FRS2$\alpha^{C4,5S}$-EGFP (right). Bar, 10 μm.

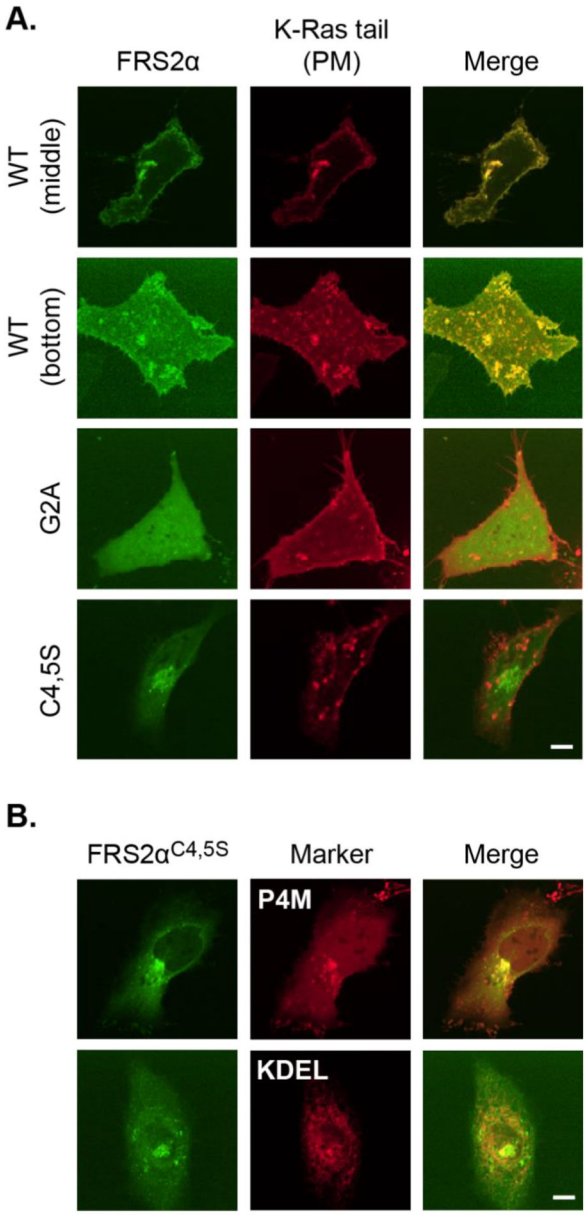

Figure 3.

Accumulation of the palmitoylation-deficient FRS2$\alpha^{C4,5S}$ mutant on the Golgi. (A) Confocal images of HeLa cells cotransfected with either WT or mutant forms of FRS2α-EGFP as indicated and the PM marker, the mCherry-K-RAS tail. (B) Confocal images of HeLa cells cotransfected with FRS2$\alpha^{C4,5S}$-EGFP and mCherry-P4M (Golgi-enriched) or mCherry-KDEL (ER marker) Bar, 10 μm.

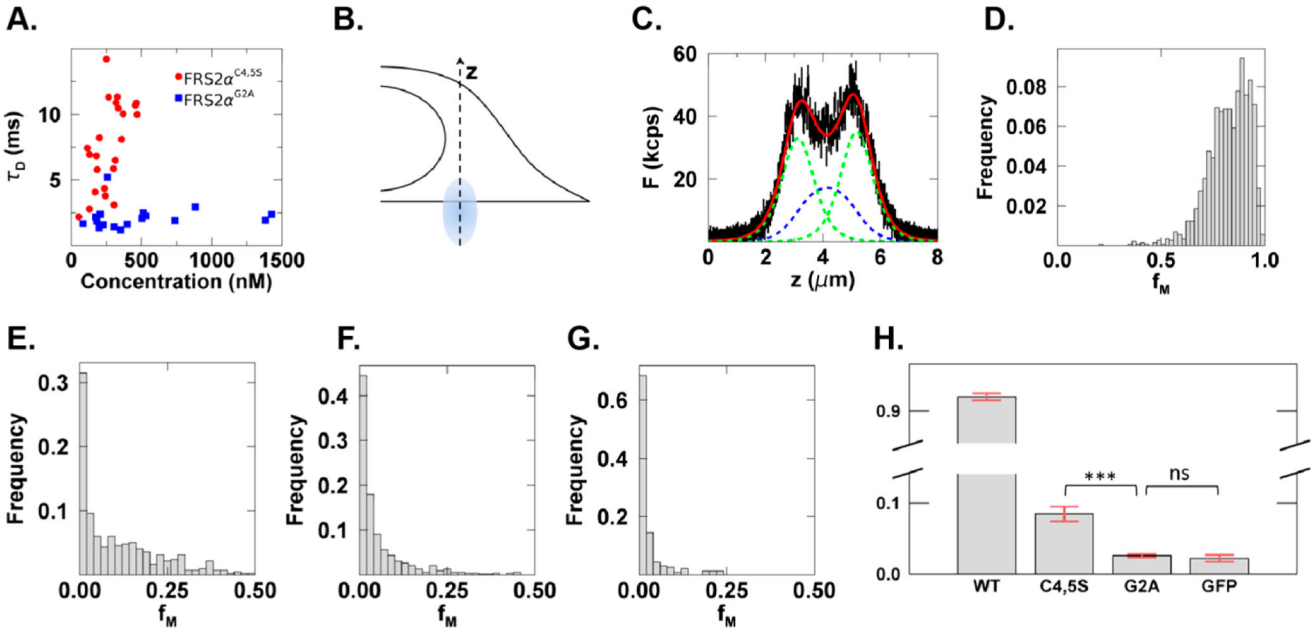

Figure 4.

FCS and z-scan characterization of cytoplasmic mobility and PM binding of FRS2α. (A) The cytoplasmic diffusion time of FRS2α^{G2A}-EGFP is concentration-independent with a mean value of 2.2 ms. In contrast, the diffusion time of FRS2$\alpha^{C4,5S}$-EGFP increases with concentration, which is indicative of transient interactions with cellular factors of a low mobility. (B) Conceptual illustration of a z-scan of the two-phot6on focus through a cytoplasmic location. (C) Z-scan intensity trace of FRS2α^{WT}-EGFP with two prominent peaks identifying protein bound to the ventral and dorsal PM. A fit identified the membrane contributions (green, dashed line) as well as the cytoplasmic component (blue, dashed line) to the total fluorescence signal (red, solid line). The ventral and dorsal PM fractions calculated from the fit are 75% and 76%, respectively. (D–G) Histograms of PM fraction of FRS2α^{WT} (D), FRS2$\alpha^{C4,5S}$ (E), FRS2α^{G2A} (F), and GFP control (G). (H) Median and its standard error of the PM fraction at low concentrations (20 to 100 nM) for FRS2α^{WT}, FRS2$\alpha^{C4,5S}$, FRS2α^{G2A}, and GFP.